Title
A Wound Healing Study on Embryonic Chick Corneas using Second Harmonic Generation Imaging

Permalink
https://escholarship.org/uc/item/3pp9f6x4

Author
Tran, Stephanie Thuy-Vy

Publication Date
2015

Peer reviewed|Thesis/dissertation

UNIVERSITY OF CALIFORNIA,
IRVINE

A Wound Healing Study on Embryonic Chick Corneas using Second Harmonic
Generation Imaging

THESIS

Submitted in partial satisfaction of the requirements
for the degree of

MASTER OF SCIENCES

in Biomedical Engineering

by

Stephanie Thuy-Vy Tran

Thesis Committee:
Professor James V. Jester, Chair
Assistant Professor Donald J. Brown
Assistant Professor Peter Lwigale

2015

TABLE OF CONTENTS

LIST OF FIGURES

LIST OF TABLES

ACKNOWLEDGMENTS

I would like to express my appreciation for my advisor and committee chair, Dr. James V. Jester for his guidance in my undergraduate and graduate research. I have learned so much from him and would not have been able to complete this thesis without his guidance and support. I would also like to thank my committee members, Dr. Donald Brown and Dr. Peter Lwigale for being supportive in my research project and for reviewing my thesis.

I would like to extend a thank you to the people in my lab who have mentored and helped me with my research. Yilu, thank you for all the training on sectioning and staining, and Dr. Mortiz Winkler, for teaching me how to do pretty much everything else in the lab. I couldn't have done it without you both!

I would also like to thank my family and friends for always supporting me in everything that I do. Special thank you to my mom, dad, brother, and sister for their support, and my dog Sammy for always keeping me company while I write.

ABSTRACT OF THE THESIS

A Wound Healing Study on Embryonic Chick Corneas using Second Harmonic
Generation Imaging

By

Stephanie Thuy-Vy Tran

Master of Science in Biomedical Engineering

University of California, Irvine, 2015

Professor James Jester, Chair

Damage or infection to the adult cornea results in scarring and loss of transparency. Since fetal tissue has been known to regenerate without scarring, we wanted to study corneal wound regeneration in an embryonic chick cornea. The avian cornea and human cornea have very different corneal collagen structures, so we also wanted to compare and identify the differences in these collagen structures. Our lab has developed a second harmonic generation optical imaging paradigm called Non-Linear Optical High Resolution Macroscopy (NLO-HRMac). This imaging technique has the ability to image large cross-sectional volumes of corneal collagen at sub micron resolution in three dimensions.

Chick embryo corneas were wounded at embryonic day (E) 7 by creating a linear incision traversing the epithelium and anterior stroma. The eyes were collected at E16, 9 days post wound (dps). Using HRMac, we were able to image a control embryonic chick cornea at E16 to determine if the cornea regenerated scar-free.

Chapter 1. Introduction

MOTIVATION

The cornea plays a vital role in our vision, as it accounts for two-thirds of the eye's total optical power. Light strikes the cornea and refracts onto the lens. The lens further refocuses the light onto the retina, which converts the light rays into impulses and sends them through the optic nerve to the brain, which then interprets them as images. If there is damage to the corneal surface, the shape of the cornea is shifted and the light refracting onto the cornea distorts vision. This results in an alteration of the cornea's refracting power. Many visual acuity problems occur when the cornea has an abnormal curvature. Damage or infection to the cornea also negatively impacts visual acuity and leads to corneal scarring after wound repair.

However, in fetal tissue, wound healing does not involve scarring. In this study, we sought to explore wound-healing regeneration of the cornea in a chick embryo. We hope to be able to visualize continuous collagen fibers using NLO-HRMac imaging of the chick cornea after being wounded in ovo. Knowing that the collagen structure of the adult chicken is significantly different than that of the human cornea, we hope to visualize collagen fiber patterns that are fully restored resembling the uninjured adult chicken cornea.

OBJECTIVES

In regards to the wounded embryonic chick corneas, my research will focus on second harmonic generation (SHG) imaging using our imaging technique developed by our lab. We will obtain two samples, four eyes, from our collaborator Dr. Peter Lwigale's lab at Rice University, who performed wounds by making linear incisions across the epithelium and anterior stroma of the cornea at E7. The wounded corneas were allowed to heal until E16, at which point the eyes were collected. We obtained two control eyes and two wounded eyes, both at E16. The corneas will be dissected, sectioned, and imaged using NLO-HRMac. We hypothesize that full restoration of collagen fiber organization will be present at E16, and no scarring or disruption of the collagen structure will be present after wounding of the embryonic tissue.

Chapter 2. Second Harmonic Generation (SHG) Imaging

INTRODUCTION TO SHG IMAGING

Second Harmonic Generation imaging (SHG) has been established as a viable microscope imaging contrast mechanism for visualization of collagen fiber structural organization. Unlike conventional microscope optics that obtains its contrast by detecting variations in optical density, path length or refractive index, SHG obtains contrasts from variations in a specimen's ability to generate second harmonic light from the incident light. SHG imaging is nonlinear and absorption-free, and for the purpose of this study, uses femtosecond lasers to generate second harmonic signals from collagen to visualize collagen organization at high spatial resolution and contrast [1]. This can be compared to fluorescent microscopy, where fluorescence and phosphorescence is used in addition to reflection or absorption. SHG imaging in contrast, is absorption free [2]. Its nonlinear optical process allows photons with the same frequency interacting with a non-centrosymetric material to generate a new photon with twice the energy, and in turn twice the frequency and half the wavelength of the initial photons. This phenomenon is referred to as frequency doubling and was first demonstrated by Franken et al in 1961 [3]. The formulation of SHG was initially described by Maria Goeppert Mayer in 1931 [4] (Figure 1).
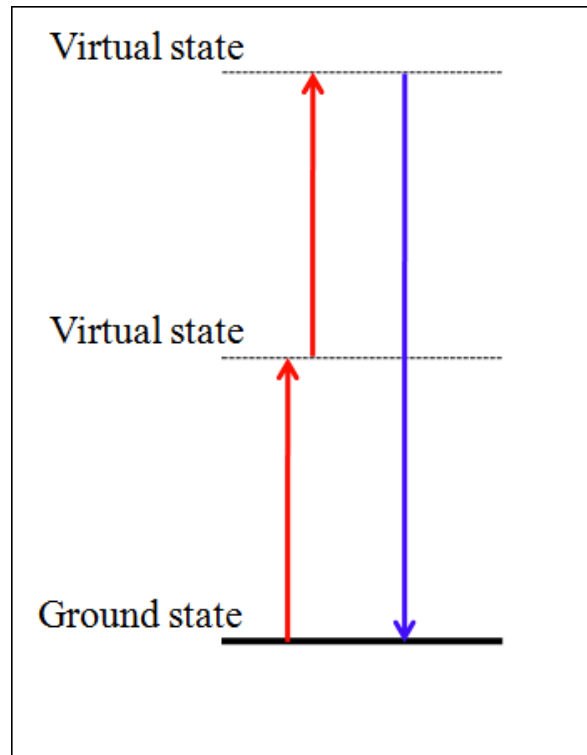
Figure 1: State diagram depicting the SHG emission process. Two incoming photons with the same frequency, shown in the red arrow combine to form a single photon with twice the frequency and therefore twice the energy and half the wavelength, shown in the blue arrow [5].

In order to generate SHG signals, ultra short laser pulses with wavelengths near the infrared regime are focused into a specimen through microscope optics [2]. These laser pulses range around several hundred femtoseconds. A small focal spot is generated in conjunction with the short pulse length and effectively focuses photons both spatially and temporally into a space volume. The energy of each pulse is small, around the order of a few hundred or dozen nanojoules. Because of spatial and temporal focusing, each pulse is associated with very high electric field strengths, inducing a polarization in the target volume by displacing subatomic charges relative to each other. The field fluctuates with the frequency of incoming light, and an oscillating polarization is induced [2]. This can be demonstrated through Maxwell's equations,

which show that such an oscillating polarization will generate its own field at double the frequency of the incoming laser light, which generates photons at exactly half the wavelength [6] (Figure 2). The mathematics behind this optical process can be described greatly in detail by Kleinman in his theory of second-harmonic generation of light [7].
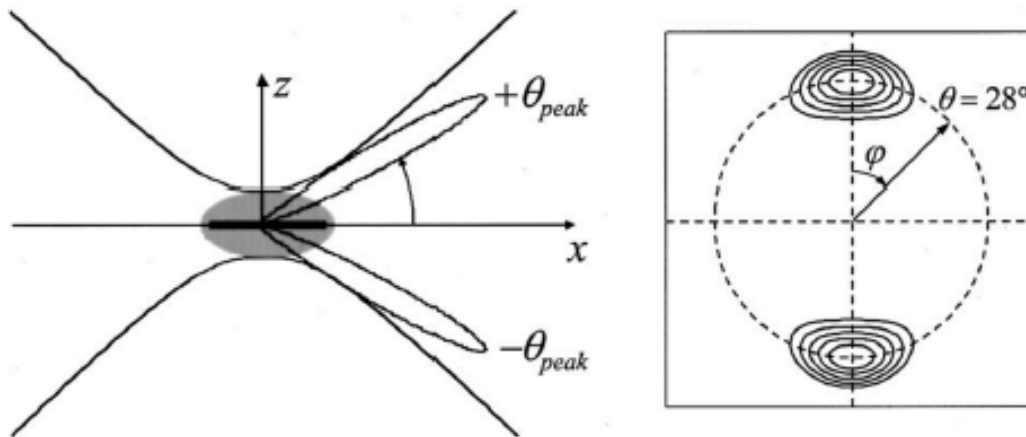
Figure 2: SHG emission characteristics in an idealized 2-D system as depicted by Moreaux [8].

APPLICATIONS

Second harmonic generation (SHG) imaging is used in the biomedical field to generate three dimensional, high-resolution images of tissues. Conventional optical microscopy uses single-photon interactions such as single-photon absorption for fluorescence imaging, whereas SHG is a multiphoton process.

The development of this nonlinear optical (NLO) technique has emerged as a powerful new tool for studying collagen organization, and is extremely useful for

applications in ophthalmology [9]. The use of ultra short laser pulses cause an oscillating polarization in molecules such as collagen, that results in the emission of light at exactly half the wavelength of the laser beam [2]. This process yields high lateral and axial resolution that allows for 3-D image acquisition through the full thickness of the cornea. Because of phase matching conditions that must be met, SHG is limited to structures that lack central symmetry. Fibrillar collagen is the only corneal structure that lacks this central symmetry, thus it is the only element in the cornea that emits an SHG signal. Because of this, imaging collagen fibers does not require staining [2]. With SHG imaging, images of individual fibers or bundles of fibers can be obtained at submicron resolution.

Furthermore, second harmonic generation microscopy can only pick up signals of collagen fibers that run roughly perpendicular to the direction of the scanning beam. During cross sectional imaging, the collagen running in plane with the section is visible, whereas the fibers running toward the observer do not generate a signal, and is seen as a black space in acquired SHG images [6].

NLO-HRMAC

An SHG-based imaging paradigm called Non-Linear Optical High Resolution Macroscopy (NLO-HRMac) developed by our lab has allowed for the generation of large scale, high resolution, three-dimensional reconstructions of corneal cross sections. In NLO-HRMac, the combination of high resolution and 3-D imaging capability of SHG creates a field of view large enough to image an entire corneal cross section. We are able to observe an entire 3-D reconstruction of collagen fibers without the need for

staining. This can be achieved by sequentially acquiring individual, overlapping image stacks to cover the desired area to be imaged. Following imaging, we digitally convert these images into a single, large mosaic. This imaging method has allowed us to study in depth, the collagen organization of the cornea in humans and various species.

Figure 3: 3-D reconstruction of embryonic chick cornea cross section. Multiple images were acquired, followed by conversion into a single large mosaic. This is one plane of the image, showing collagen fiber organization of the chick cornea at E16.

Chapter 3. Corneal Structure in Humans

INTRODUCTION

The cornea is a transparent thin layer that covers the surface of the eye. In humans, the cornea is aspheric in shape and has a thickness of about 500μm. The diameter of the cornea is about 11.5mm and its refractive power averages 43 diopters. The cornea contributes most of the eye's focusing power. Because transparency is of prime importance, the cornea does not contain any blood vessels. It receives nutrients from tear fluid from the outside surface, and from the aqueous humor through the inside surface, along with neurotrophins supplied by nerve fibers that innervate the cornea. 5 layers make up the cornea. From anterior to posterior, these layers are the epithelium, Bowman's membrane, the stroma, Descemet's membrane, and the endothelium (Figure 4).
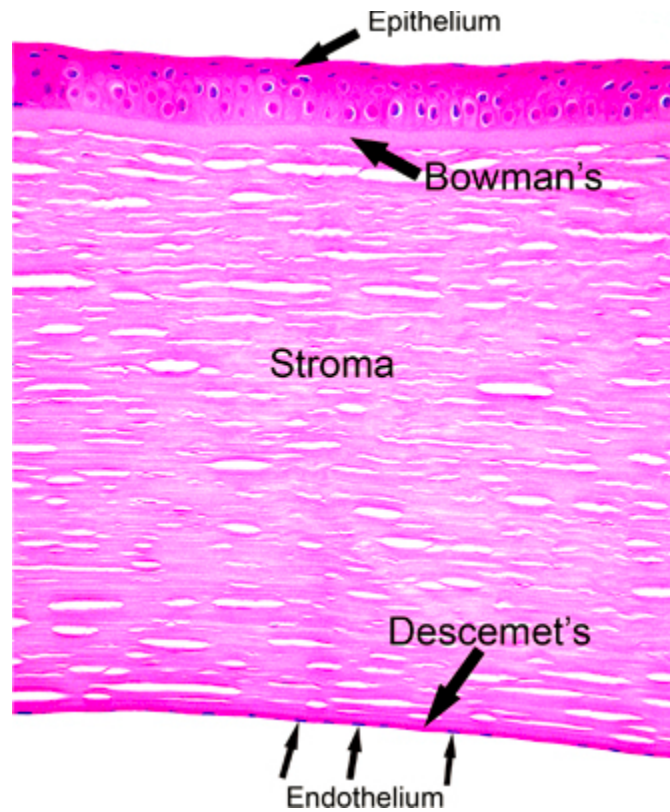
Figure 4: Histology slide representing 5 layers of the human cornea [10]

Epithelium

The corneal epithelium serves as the first barrier of the cornea, and is an exceedingly thin multicellular epithelial tissue layer of fast-growing and regenerating cells. It is comprised of 5-7 cell layers and is firmly attached to the underlying stroma [11]. The corneal epithelium, like most epithelia, continually sheds cells into the tear film to maintain pathogen barrier function and reduce bacterial infection [12].

Bowman's Layer

Bowman's layer is a tough layer composed of mainly type I collagen fibrils, laminin, perlecan and other heparin sulfate proteoglycans that protect the corneal stroma. It is 8-12μm thick and is acellular; however keratocytes are found in Bowman's layer during early development [13]. This layer is a visible indicator of ongoing stromal-epithelial interactions in the human and studies have shown that there has been controversy over the role and function of this layer. There has been little evidence showing a critical physiological function of Bowman's layer [13]. Studies also suggest that removal of Bowman's layer does not measurably alter the mechanical properties of the cornea [14].

Stroma

The stroma, which is the primary layer we will focus on in this study, is a thick transparent middle layer of collagen. It comprises 90% of the cornea's total thickness. The stroma is approximately 78% water, 15% collagen, and 7% non-collagenous proteins, proteoglycans, and salts [15]. The structure of the collagen will be explained further in detail below. Between the collagen fiber bundles in the stroma are cells called keratocytes that are involved in general maintenance and repair. Keratocytes are sparsely filled between collagen fibers, and occupy about 10% of the cornea. These keratocytes play an important role in the wound healing response, where proliferation and migration of keratocytes and differentiation to fibroblasts and myofibroblasts can lead to corneal scarring of the stroma [16].

Descemet's Membrance

Below the stroma is Descemet's membrane, a thick basement membrane that is built by the cells of the flat squamous epithelium, measuring about 5-10µm thick [17]. It is composed of a type IV collagen, a non-fiber forming collagen that is different from the collagen that comprises the stroma [18].

Endothelium

The fifth and final corneal layer, the endothelium, is comprised of flattened, mitochondria rich cells that line the posterior surface of the cornea and face the anterior chamber of the eye. The endothelial cells possess a water pump that keeps the cornea in a constant state of dehydration, helping to prevent corneal edema [10]. These endothelial cells do not regenerate [19].

STROMAL COLLAGEN STRUCTURE

As mentioned, the primary focus for this study will be the corneal stroma. The mechanical strength and shape of the cornea is dependent on this layer, as this layer makes up 90% of the total corneal thickness. Of the five anatomic layers of the cornea, only Bowman's layer and the stroma contain collagen fibrils, and these layers thus provide the majority of the cornea's tensile strength [16]. The corneal stroma is a collection of type I collagen fibrils, accounting for 70% of the corneal total dry weight [20]. These collagen fibrils have uniform diameter of approximately 31-34nm and assemble to form long fibers, known as lamellae [21]. Three hundred to five hundred lamellae traverse the entire cornea from limbus to limbus and are stacked with angular

offsets; and this orientation becomes increasingly more random in the anterior stroma [22]. The size, spacing and stability of the fibrils are regulated by non-fibrillar collagen and proteoglycans found in the interfibrillar matrix [23]. Each collagen fiber is approximately 1-2µm thick and 10-200µm wide [24]. The organization of these collagen fibers creates a transparent layer that influences corneal shape, which in turn plays an important role in determining visual acuity. Our lab has begun to quantify the macrostructure of the human cornea, and demonstrated a link between the degree of collagen lamellar branching and corneal compliance [2]. Based on these findings, we proposed that collagen lamellar branching and anastomosing stabilizes corneal biomechanics and controls corneal shape in the human cornea.

Chapter 4. Corneal Structure of Embryonic Chicks

INTRODUCTION

Chick embryos have been widely used as models to study development and wound healing. Chick embryos post fertilization develops within 21 days, with 46 stages of development according to Hamburger and Hamilton staging system [25]. This system allows us to use consistent time points to compare development of the chick embryo. In this particular study, it allowed us to study the cornea in the chick embryo and its ability to regenerate the cornea after being wounded at a specific time point.

The collagen organization of the adult chicken cornea and subsequently avian corneas is significantly different than that of the human cornea [26]. The adult chicken cornea also has Bowman's layer [13]. The stroma in the adult chicken cornea is comprised primarily of water, collagen, glycosaminoglycans and stromal fibroblasts [27, 28]. The thickness of the adult chicken corneal stroma is 200µm and consists of layers that are 2 to 4µm thick, which lie roughly parallel to the corneal surface [26]. The collagen fibers within each layer are oriented in the same direction approximately at right angles to one another, with an angular shift in a clockwise direction proceeding from anterior to posterior layers [26]. This orientation is the same in both the right and left eye.

DEVELOPMENT OF THE EMBRYONIC CHICK CORNEA

The primary corneal stroma is produced by the corneal epithelium and then deposited beneath the epithelial surface in an orthogonal pattern. The acellular primary corneal stroma serves as a scaffold for mesenchymal cells to invade and produce the secondary corneal stroma [26]. During the developing stages of the embryonic chick cornea, the primary corneal stroma at E5 swells from a thickness of 10μm to about 60μm and is invaded by mesenchyme. By E6, the entire corneal stroma is about 110μm thick. The orthogonal layers of collagen in the posterior 100μm of the invaded stroma show no angular displacement. By E7, the corneal stroma is about 170μm thick, and the orthogonal layers of collagen in the posterior 120μm show no angular displacement with respect to the choroid fissure axis [26]. However, the orthogonal layers in the remaining 40μm of the invaded stroma show a clockwise angular displacement. By E14, the cornea reaches the thickness of 200μm and is invaded throughout by mesenchyme. Only a narrow 1-2μm thick zone beneath the epithelium remains not invaded. Due to dehydration, the thickness of the corneal stroma begins to compact and decrease. This results in a cornea with an angular displacement in the anterior 150μm portion of the stroma at about 1.4° per μm, with each layer being 2-4μm thick, and no angular displacement in the posterior 50μm of the stroma (Figure 5).
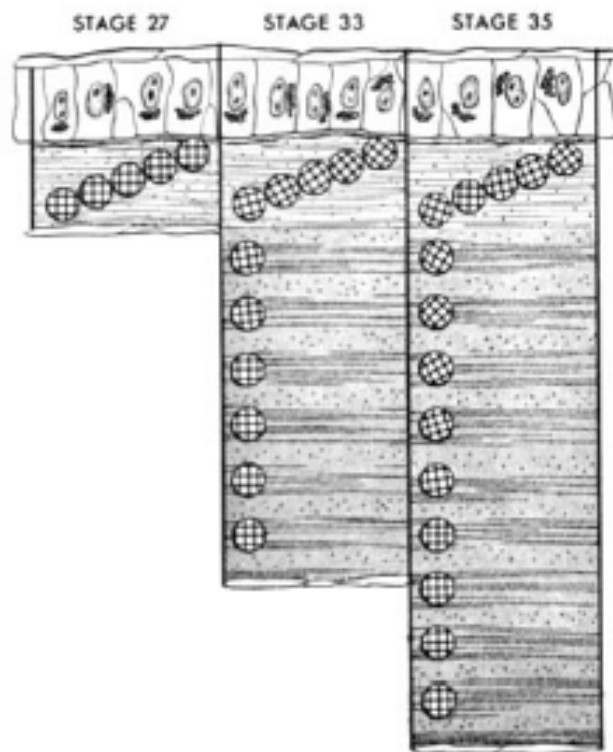
Figure 5: Three stages in the development of the corneal stroma illustrated by Trelstad & Colulombre. Two planes of section have been diagrammed. The circles with orthogonal grids, representing a plane parallel to the corneal surface, have been superimposed on the diagram representing a section perpendicular to the corneal surface. Each circle illustrates the orthogonal orientation of the stromal matrix at that particular level in the stroma [26].

The development of the embryonic chick cornea has been studied using electron microscopy, in which a fully formed primary stroma identical to the adult chicken is present [26]. The organization of the primary corneal stroma has been thought to contain the complex pattern organization of the adult cornea. It is believed that the primary stroma may then dictate the pattern and organization of the adult chicken stroma. Trelstad and Colombre proposed that the morphogenesis of this three dimensional architecture with an acellular matrix may be a self-assembly process [26].

15

HUMAN VS. AVIAN CORNEAL STRUCTURE

Human corneas exhibit a completely different collagen organizational structure than that of an avian cornea, particularly the adult chicken. While the avian cornea is comprised of orthogonally arranged collagen fibers with an angular shift from anterior to posterior, these layered collagen fibers are replaced by more dynamic fiber bundles in human corneas [29]. These fiber bundles can be oriented in different directions within the same plane and are not limited an individual plane or layer (Figure 6). These bundles also weave in and out of the focal plane often, causing a visualized dashed appearance on an SHG image. In avian corneas, adjacent layers are highly interconnected by frequent branching and anastomosing, creating a structure that resembles the look of chicken wire [29] (Figure 7). The thickness of the adult chicken cornea is 200μm, which is less than half the thickness of the human cornea of 500μm.

Viewing the embryonic chick cornea en face, as we move through the thickness of the stroma, there is a gradual angular shift clockwise. This can be visualized in the FFT images of the control chick embryo at E16 (Figure 9).
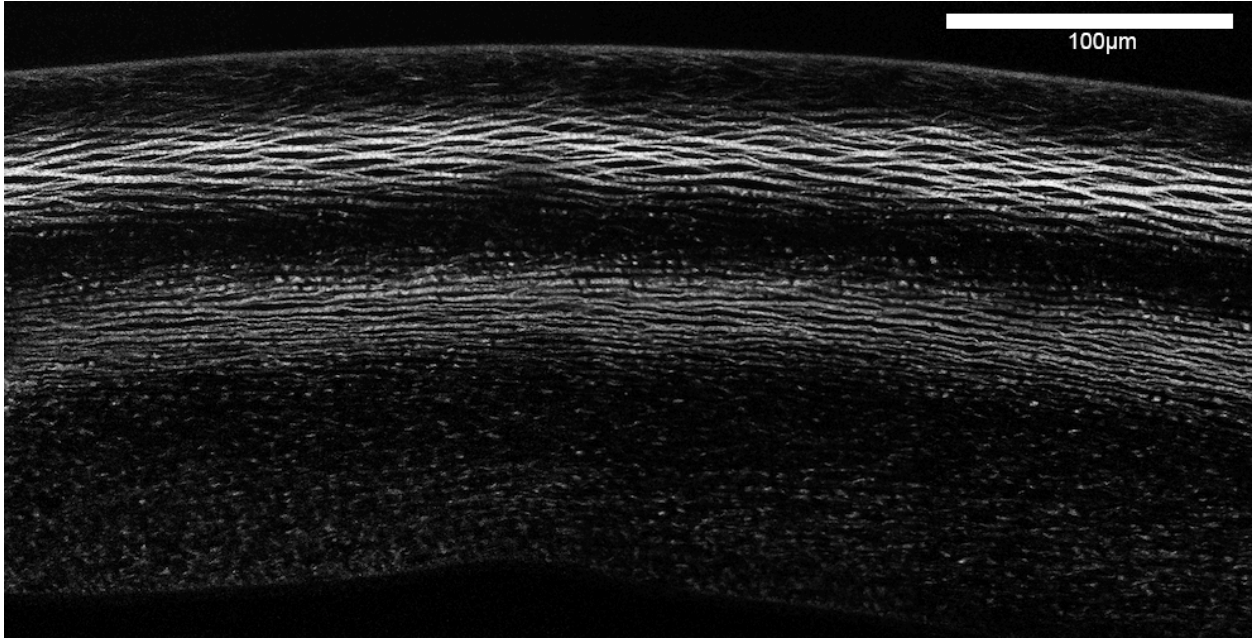
Figure 6: NLO-HRMac cross sectional image of adult chicken cornea.
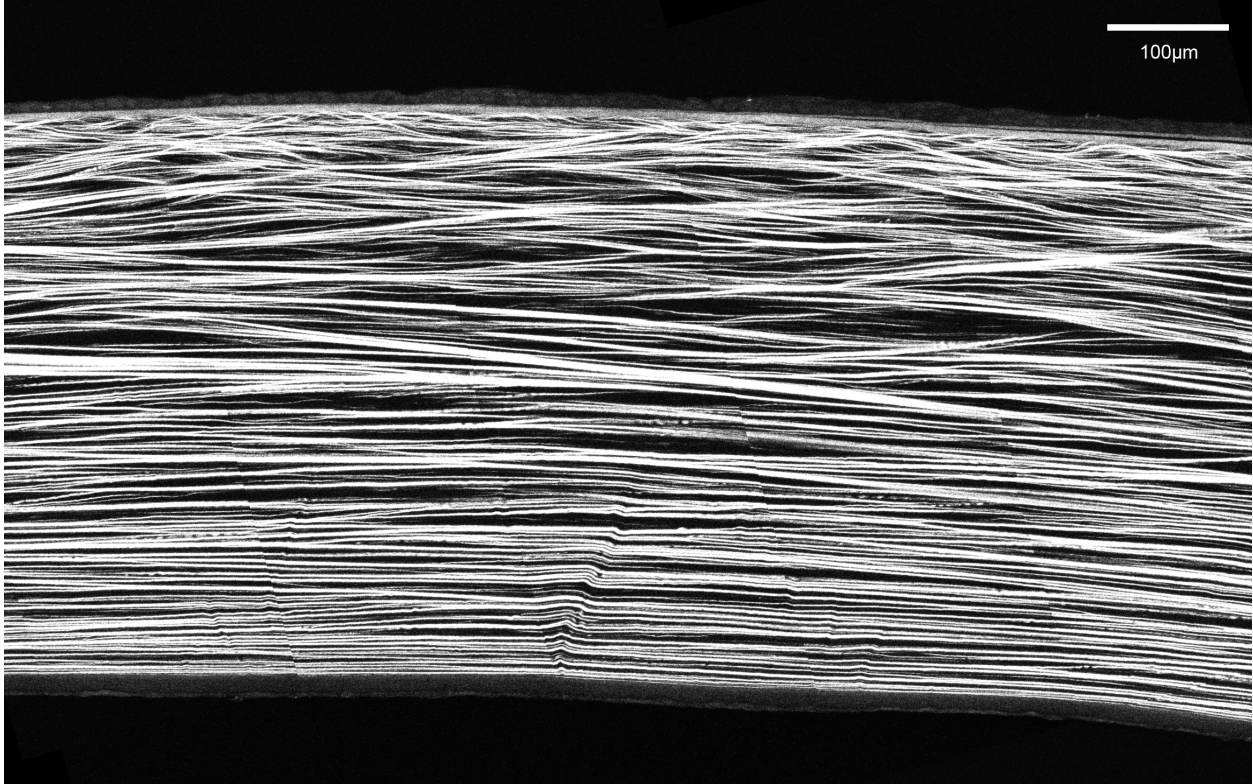

Figure 7: NLO-HRMac cross sectional image of adult human cornea.

Chapter 5. Restoration of Normal Collagen Fiber Organization Following Embryonic Wound Healing

INTRODUCTION

The structural properties of the cornea are essential to its function as a resilient, yet transparent, barrier to intraocular injury [16]. Damage or infection of the adult corneal stroma results in scarring and loss of transparency in the cornea [30, 31]. Fetal tissues regenerate rapidly with no detectable scar formation [32]. Recent studies have shown that wounded embryonic corneas regenerate without formation of scar tissue, thus preserving corneal transparency [33]. Since avian corneas have a unique, rotational and orthogonal collagen fiber organization previously defined by Trelstad, the purpose of this study was to determine whether embryonic wound healing recapitulated the normal avian corneal stromal organization. We investigated whether normal stromal collagen fiber patterns are fully restored after embryonic wound healing in chick corneas.

MATERIALS AND METHODS

Tissues

Animal studies were approved by the Institutional Animal Care and Use Committee (IACUC) of Rice University. Fertilized White Leghorn chicks (*Gallus gallus domesticus*) were obtained from Texas A&M Poultry Center (College Station, TX) and prepared using a technique to increase accessibility to late-stage chicken embryos for in

ovo manipulations [33]. Briefly, eggs were incubated at 38°C and processed through a series of manipulations to remove the extra embryonic membranes and enable access to the right eye of (E) 7 embryos in ovo [33].

Sample Preparation

On embryonic day E7, chick corneas were wounded by making a linear incision traversing the epithelium and anterior stroma [33] (Figure 8). A micro-dissecting knife (30° Angled Micro-Dissecting Knife; Fine Science Tools, Foster City, CA) was used to create the wound, and the incision was made across the cornea with lacerations traversing the corneal epithelium, basement membrane, and anterior stroma [33]. Ringer's solution containing penicillin (50 U/mL) and streptomycin (50 U/mL) was added to the embryos after wounding and the eggs were sealed with transparent tape and reincubated [33]. At E16, 9 days post wound (dpw), the wounded and control eyes were collected, and the corneas were dissected.
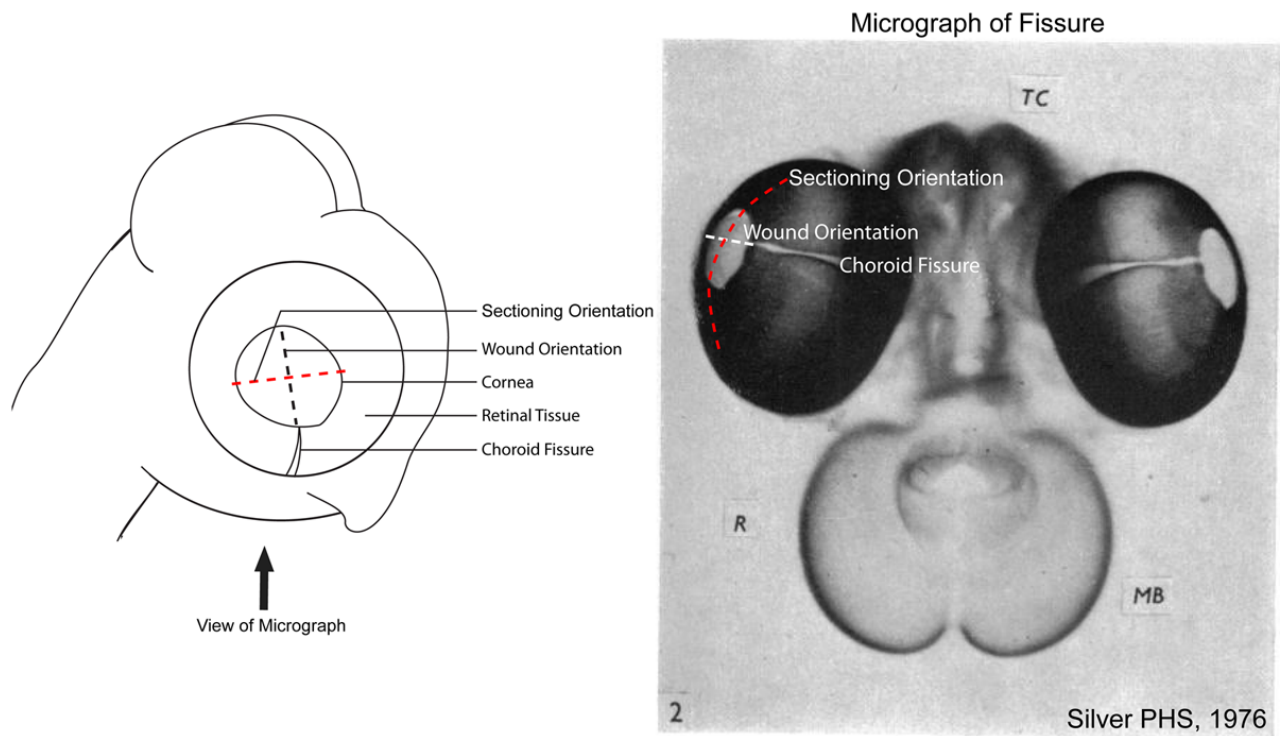
Figure 8: Orientation of wound in relation to choroid fissure, prepared by collaborating lab: Lwigale and Spurlin. An incision was made traversing the epithelium and anterior stroma. The sectioning direction was made perpendicular to the wound.

In two eyes, one wounded and one control at E16, 1.5mm corneal buttons were dissected from the central cornea using a trephine and stored in 2% paraformaldehyde in PBS for en-face, through-focus, 3-D second harmonic generation imaging. Two additional eyes, one wounded and one control at E16, were used for cross sectional imaging. The unfused Choroid Fissure in the chick embryo at E7 was used as a marker to determine the orientation of the wound. By E16, the fissure is partially closed, but was still used to determine the orientation of the wound across the cornea. The corneas were dissected from the eyes of the chick embryos at E16 using a scalpel blade. These corneas were then embedded with the wound in the vertical position in low melting point agarose (NuSieve GTG, Lonza, Rockland, ME). Serial full-width cross-

sections of 250µm thickness were sectioned perpendicular to the wound using a vibratome (Vibratome 1500, Intracel Ltd, Shepreth, UK) and stored in 2% paraformaldehyde in PBS.

NLO-HRMac Imaging

The 1.5mm buttons and a 250µm cross-section of the central cornea were scanned with a Zeiss LSM 510 meta microscope (Carl Zeiss Imaging, Thornwood, NY). The 1.5mm buttons were imaged through the entire thickness using nonlinear optical high-resolution macroscopy imaging (NLO-HRMac) at submicron resolution. These images were collected with a step size of 1µm intervals. For these through-focus en face images, a 40x/ 1.1 NA objective was used that resolves the microstructure of the cornea easily, with images at .44 µm per pixel. Each image represents a 225 x 225 µm area. Three different through focus data sets were taken in different areas around the central cornea. To image the entire section of the cornea across the full corneal diameter, images were acquired with a 20x objective using Zeiss MultiTime macro function. The HRMac images were used to determine continuity of collagen fibers after healing.

Image Processing

En face images were combined to create a stack of images from anterior to posterior. Fast Fourier Transforms (FFT's) of en face images were then generated using custom-written software developed by our lab for ImageJ version 1.39 (National Institute of Health, http://rsb.info.nih.gov/ij/). The generated FFT's were then loaded

21

onto Amira 5.2 (Visage Imaging, Carlsbad, CA) and painting was performed over the spokes to create an FFT construction. This construction shows collagen fiber orientation and clockwise rotation throughout the entire stack (Figure 9 & 10, Panel E).

Following cross-sectional imaging, images were converted from Zeiss's native .LSM format and saved as a series of .TIFF files using the LSM toolbox plugin for ImageJ. Stitching was accomplished through a combination of ImageStitch plugin and custom written imageJ macro written by our lab. These plugins combined the individual .TIFF files into mosaics, using registration algorithms to correct for image misalignments that may have occurred from stage movements or sample drift. The stitched images were combined into a single plane .TIFF file for the cross sectional image of control and wounded corneas (Figure 11).

Layer Counting and Angle Determination

The en face images that were converted to FFT's were stacked to about 80 layers, and the amount of rotations in each layer was manually counted by clicking through the stack. The resulting counts were recorded on to an excel spreadsheet, counted in 10 layer intervals. The intervals were summed up and repeated for four trials, and averaged. This was done for each of the three images that were scanned. The resulting 3 numbers were averaged again, to determine the number of layers for the control and wounded corneas. The standard deviation was also calculated for the layers. (Table 1).

To determine the angle of rotation of the collagen fibers, the angle measure tool from ImageJ was used to measure the angle from the first layer to the last layer in the

FFT stack. The rotation angle was also taken four times, and the mean and standard deviation for these measurements were also calculated (Table 1).

	Control	Wound
Layer Count	60.2 ± 2.4	57.8 ± 4.0
Angle of Rotation	166° ± 5	161° ± 4

Table 1: Layer count and angle of rotation, averaged over 3 images with 4 trials of counting per image.

Results

The wounds were made on the right eyes of the chick embryos at E7, and this particular time was chosen because at E7, the three cellular layers of the cornea are formed [34]. At this time point, there are expressed characteristic markers in the epithelium [35], stroma [36, 37], and endothelium [35]. This allowed us to better observe wound healing characteristics in the chick embryo cornea.

At E16, there appeared to be no difference in collagen organization between the control and wounded corneas. Number of layers and rotation angles appeared similar in both control and wounded corneas (60 layers, 166° control vs. 58 layers, 161° wounded) (Figure 9 &10), and continuity of fibers was fully reestablished (Figure 11). To better visualize the angular rotation from anterior to posterior, the FFT's were computed, assembled as image stacks, and rendered in 3-D (Figure 9 & 10, Panel E). Each spoke represents the predominant directionality of collagen fibers within each layer.
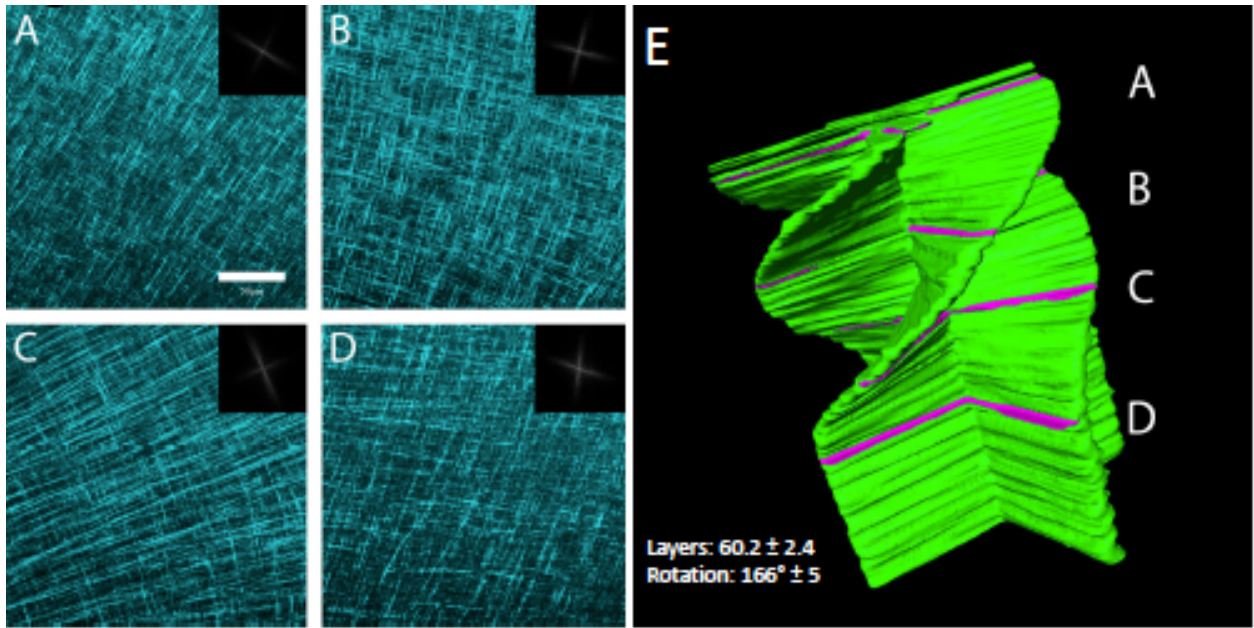
23

Figure 9: The panel on the left shows four different layers taken from an en face scan of the control embryonic chick cornea. On the upper right hand corner of each subpanel, FFT's of each image were computed to show the orientation of the collagen fibers. On the panel on the right, the FFT constructions show the corresponding layers (A-D) that are highlighted in magenta. Number of layers and rotation angles are shown in the bottom left hand corner of panel (E)

Figure 10: The figure above shows the same image analysis as Figure 9 but for the wounded cornea. The panel on the left shows four different layers taken from an en face scan of the wounded embryonic chick cornea. On the upper right hand corner of each subpanel, FFT's of each image were computed to show the orientation of the collagen fibers. On the panel on the right, the FFT constructions show the corresponding layers (A-D) that are highlighted in magenta. Number of layers and rotation angles are shown in the bottom left hand corner of panel (E).
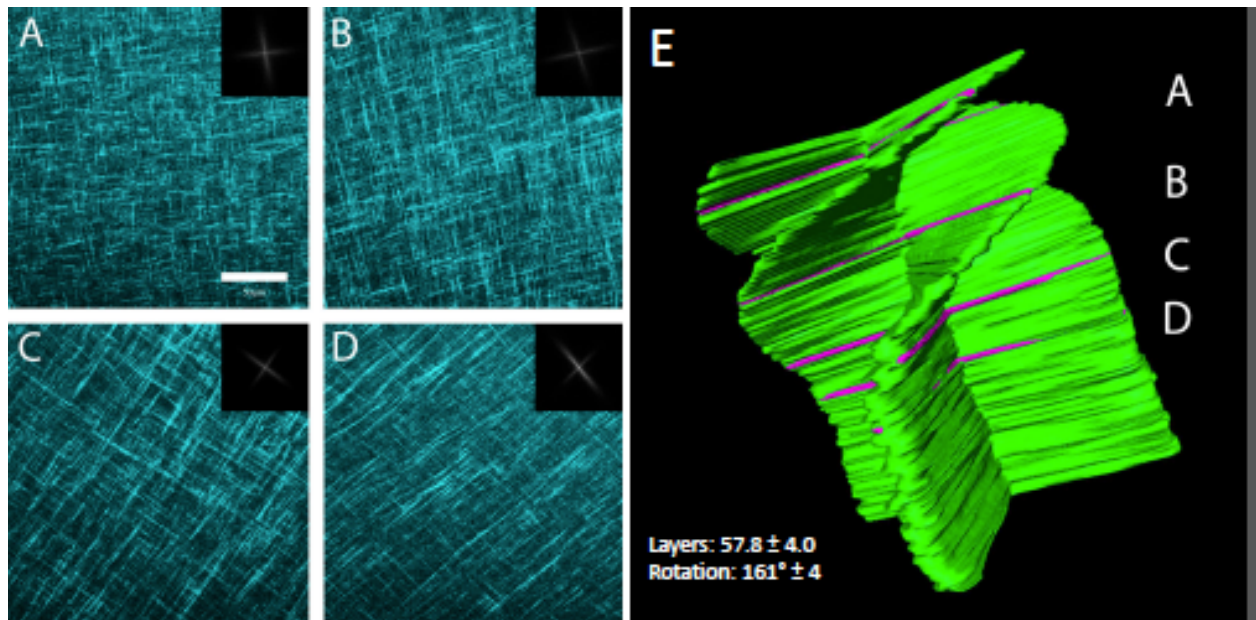
24

For the cross sectional images of the chick corneas, no breaks in collagen fiber patterns were visualized. Full continuous collagen fibers were seen in both the wounded and control cornea cross sections (Figure 11). A close-up view of each image also further emphasizes the formation of continuous fibers, and recapitulation of the stromal collagen fiber pattern that is visualized in the chicken. For cross sectional images, only fiber bundles in plane are shown in the NLO-HRMac images whereas fiber bundles perpendicular to the plane do not emit an SHG signal. Dark bands are indicative of collagen fibers orienting toward the observer, and the banding is caused by the rotation of the collagen fibers that are present in avian corneas.
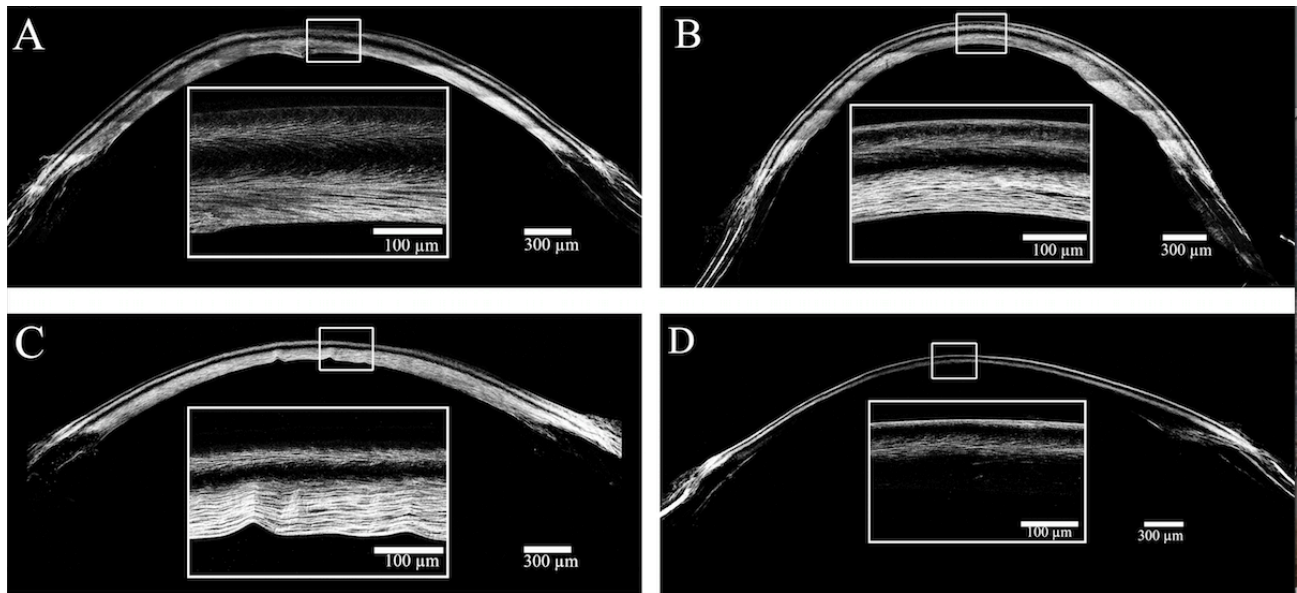

Figure 11: Cross section images of two control (A,C) and two wounded (B,D) embryonic chick corneas at E16. A zoomed in high resolution image below each cross section shows fiber continuity. Panel D shows a different scanning orientation of the cross section, making the section appear thinner; however continuous collagen fibers are still visualized.

Discussion

Using a technique recently developed to access late-stage chick embryos in ovo [33], embryonic wounded corneas were collected 9 dpw and scanned using NLO-HRMac to investigate stromal collagen regeneration potential. These data suggest that the wound that was created at E7 did not negatively affect the deposition of collagen layers at E16. The data also suggests that during embryonic wound healing, the normal collagen fiber architecture in the embryonic chick cornea is fully restored. The implication here is that embryonic wound healing in the chick cornea is capable of restoring normal corneal collagen fiber organization that is apparently identical to the adult, uninjured cornea.

Our collaboration with the Lwigale lab at Rice University shows further analysis of nonfibrotic corneal regeneration post wounding. By collecting wounded corneas between E7 and E18, they had analyzed for apoptosis, cell proliferation, staining of ECM components, and corneal innervation. Their results show that corneal wounds were fully re-epithelialized by 11dpw with no visible scars [33]. There were also no differences in number of cells undergoing apoptosis between wounded and control corneas [33]. The embryonic chick corneal wounds resulting from linear incisions traversing the epithelium and anterior stroma retract until 3dpw, after which they undergo re-epithelialization that is completed at approximately 11dpw [33]. This retraction can be explained from the growth phase during the early stages of avian ocular development, which is dependent on intraocular pressure (IOP) [38]. This further confirms that embryonic chick corneas exhibit scar free, or nonfibrotic regeneration after wounding.

With the visualization of the continuous collagen fiber that is consistent with the adult chicken cornea in combination with the analysis of apoptosis, cell proliferation, and corneal innervation [33], we can conclude that the cornea was restored to recapitulate the adult chicken corneal structure. However, there are visualized differences in the control and wounded cross sectional images, which are seen through a different scanning orientation of the cornea. In images of the wounded and control corneas, the orientation at which D was scanned in Figure 11 was slightly off compared to A, B, and C. This is shown by the dark bands on the image, making D appear as a thinner section of the cornea, when in actuality it is only oriented differently towards the scanning beam due to sectioning. Future experimentation will include sectioning ability that allows for more precise orientation and show visualization of collagen fiber bands consistent across control and wounded corneas. Despite the difference in orientation, the wounded corneas show no fiber discontinuity across in the region of the wound, even though the section appeared thinner (Figure 11, Panel D). En face images are unaffected by this orientation as the rotation is seen throughout the entire stack. The wounded and control corneas showed very similar angles of rotation, number of layers, and FFT constructions (Figure 9 & 10).

Chapter 6. Conclusions and Future Directions

This wound healing study was important to visualize a fully regenerated cornea that was wounded at E7, when all three major layers of the cornea have developed in the chick embryo. At this time, the epithelium, stroma, and endothelium are all present, making it an ideal time point to create the wound. 9 days after the wound at E16, we were able to visualize a fully restored embryonic chick cornea with no detectable scar formation using NLO-HRMac imaging.

In adult corneal wounds, collagen lamellae are frequently destroyed during wound healing. Corneal scar tissues are characterized by the presence of disorganized collagenous matrix with irregular fibril spacing and larger fibril diameters [39]. It would be extremely helpful to understand the mechanisms of embryonic wound healing for the future application of procedures such as LASIK or PRK, where the cornea is ablated.

Future studies would include experimentation of different time points after wounding the chick cornea. Because of the small number of samples, further experimentation with multiple samples and multiple time points would be needed to confirm these results and better identify the mechanisms of embryonic wound regeneration. It would be interesting to see different images of wound healing taking place in the collagen fibers 3 days post wound, 5 days post wound, and before hatching.

On a further level, the collagen organization of the human cornea allows for biomechanically interesting features. The increase in corneal thickness from the central stroma to the periphery influences the local organization of the biomechanical behavior of the tissue [11]. While the human (and mammalian) corneas show collagen fibers

bundles that form highly interconnected, continuous, stabilizing structure, avian corneas show frequent branching and anastomosing of fibers, which form a collagen structure resembling that of chicken wire. The differences in collagen structures still however create a functional and transparent cornea that is able to successfully refract light onto the retina and determine visual acuity.

References

1. Campagnola, P.J. and L.M. Loew, *Second-harmonic imaging microscopy for visualizing biomolecular arrays in cells, tissues and organisms.* Nat Biotechnol, 2003. **21**(11): p. 1356-60.

2. Winkler, M., et al., *Nonlinear optical macroscopic assessment of 3-D corneal collagen organization and axial biomechanics.* Invest Ophthalmol Vis Sci, 2011. **52**(12): p. 8818-27.

3. Franken, P., Hill, A., Peters, C. & Weinreich, G, *Generation of optical harmonics.* Physical Review Letters 1961. **7**: p. 118-119.

4. M, G.-M., *Über Elementarakte mit zwei Quantensprüngen.* Annals of Physics, 1931. **9**(3): p. 273–95.

5. Sobarwiki. *Energy Level Scheme of a Second Harmonic Generation Process.* 2013.

6. Winkler, M., *(Re-)Discovering A Blueprint Of The Cornea: Structural, Biomechanical, Evolutionary and Developmental Perspectives*, I. University of California, Editor. 2014.

7. Kleinman, D., *Theory of second harmonic generation of light.* Physical Review, 1962. **128**(4): p. 1761.

8. Moreaux, L., et al., *Membrane imaging by simultaneous second-harmonic generation and two-photon microscopy.* Opt Lett, 2000. **25**(5): p. 320-2.

9. Han, M., G. Giese, and J. Bille, *Second harmonic generation imaging of collagen fibrils in cornea and sclera.* Opt Express, 2005. **13**(15): p. 5791-7.

10. Meeney, A. and H.S. Mudhar, *Histopathological reporting of corneal pathology by a biomedical scientist: the Sheffield Experience.* Eye (Lond), 2013. **27**(2): p. 272-6.

11. Ruberti, J.W.R., A.S; Roberts, C.J, *Corneal Structure and Function.* Corneal Biomechanics and Biomaterials, 2011. **13**: p. 269-295.

12. Streilein, J.W., et al., *Anterior chamber-associated immune deviation, ocular immune privilege, and orthotopic corneal allografts.* Transplant Proc, 1999. **31**(3): p. 1472-5.

13. Wilson, S.E. and J.W. Hong, *Bowman's layer structure and function: critical or dispensable to corneal function? A hypothesis.* Cornea, 2000. **19**(4): p. 417-20.

14. Seiler, T.M., M; Sendler, S; Bende T, *Does Bowman's layer determine the biomechanical properties of the cornea?* Refract Corneal Surg, 1992. **8**(2): p. 139-142.

15. Maurice, D., *The cornea and sclera.* The Eye, 1984: p. 1-158.

16. Dupps, W.J., Jr. and S.E. Wilson, *Biomechanics and wound healing in the cornea.* Exp Eye Res, 2006. **83**(4): p. 709-20.

17. Pavelka, M.R., J, *Descemet's Membrane.* Functional Ultrastructure, 2010: p. 185-185.

18. Tamura, Y., et al., *Tissue distribution of type VIII collagen in human adult and fetal eyes.* Invest Ophthalmol Vis Sci, 1991. **32**(9): p. 2636-44.

19. Schwartzkopff, J., et al., *Regeneration of corneal endothelium following complete endothelial cell loss in rat keratoplasty.* Mol Vis, 2010. **16**: p. 2368-75.

20. Meek, K.M. and C. Boote, *The use of X-ray scattering techniques to quantify the orientation and distribution of collagen in the corneal stroma.* Prog Retin Eye Res, 2009. **28**(5): p. 369-92.

21. Daxer, A., et al., *Collagen fibrils in the human corneal stroma: structure and aging.* Invest Ophthalmol Vis Sci, 1998. **39**(3): p. 644-8.

22. Komai, Y. and T. Ushiki, *The three-dimensional organization of collagen fibrils in the human cornea and sclera.* Invest Ophthalmol Vis Sci, 1991. **32**(8): p. 2244-58.

23. Zimmermann, D.R., et al., *Type VI collagen is a major component of the human cornea.* FEBS Lett, 1986. **197**(1-2): p. 55-8.

24. Winkler, M., et al., *Three-dimensional distribution of transverse collagen fibers in the anterior human corneal stroma.* Invest Ophthalmol Vis Sci, 2013. **54**(12): p. 7293-301.

25. Hamburger, V. and H.L. Hamilton, *A series of normal stages in the development of the chick embryo.* J Morphol, 1951. **88**(1): p. 49-92.

26. Trelstad, R.L. and A.J. Coulombre, *Morphogenesis of the collagenous stroma in the chick cornea.* J Cell Biol, 1971. **50**(3): p. 840-58.

27. Coulombre, A.J., *Experimental Embryology of the Vertebrate Eye.* Invest Ophthalmol, 1965. **4**: p. 411-9.

28. Anseth, A., *Glycosaminoglycans in the developing corneal stroma.* Exp Eye Res, 1961. **1**: p. 116-21.

29. Winkler, M.S., G; Tran, S.T; Xie, Y; et al., *A Comparative Study of Vertebrate Corneal Structure: The Evolution of a Refractive Lens.* Invest Ophthalmol Vis Sci, 2015. **56**: p. 2764-2772.

30. Ghiasi, H., et al., *The role of natural killer cells in protection of mice against death and corneal scarring following ocular HSV-1 infection.* Antiviral Res, 2000. **45**(1): p. 33-45.

31. Hassell, J.R., et al., *Proteoglycan changes during restoration of transparency in corneal scars.* Arch Biochem Biophys, 1983. **222**(2): p. 362-9.

32. Colwell, A.S., M.T. Longaker, and H.P. Lorenz, *Mammalian fetal organ regeneration.* Adv Biochem Eng Biotechnol, 2005. **93**: p. 83-100.

33. Spurlin, J.W., 3rd and P.Y. Lwigale, *Wounded embryonic corneas exhibit nonfibrotic regeneration and complete innervation.* Invest Ophthalmol Vis Sci, 2013. **54**(9): p. 6334-44.

34. Lwigale, P.Y., P.A. Cressy, and M. Bronner-Fraser, *Corneal keratocytes retain neural crest progenitor cell properties.* Dev Biol, 2005. **288**(1): p. 284-93.

35. Takahashi, I., et al., *Immunohistochemical analysis of proteoglycan biosynthesis during early development of the chicken cornea.* J Biochem, 1999. **126**(5): p. 804-14.

36. Funderburgh, J.L., B. Caterson, and G.W. Conrad, *Keratan sulfate proteoglycan during embryonic development of the chicken cornea.* Dev Biol, 1986. **116**(2): p. 267-77.

37. Gealy, C., et al., *Actin and type I collagen propeptide distribution in the developing chick cornea.* Invest Ophthalmol Vis Sci, 2009. **50**(4): p. 1653-8.

38. Neath, P., S.M. Roche, and J.A. Bee, *Intraocular pressure-dependent and -independent phases of growth of the embryonic chick eye and cornea.* Invest Ophthalmol Vis Sci, 1991. **32**(9): p. 2483-91.

39. Nishida, T., *Corneal Healing Responses To Injuries And Refractive Surgeries*, ed. K. Publicatons. 1998, New York, NY.